Desalination and Water Treatment
www.deswater.com

doi: 10.5004/dwt.2021.27216

225 (2021) 252–264
June

Descriptive and predictive modelling of nitrates presence in water and its turbidity by unconventional experimental design after bentonite adsorption treatment

Nadia Ramdani[a], Mokhtar Bounazef[b,*]

[a]*Chemistry, Applications of Plasma, Electrostatics and Electromagnetic Compatibility, Faculty of Technology, Djillali Liabes University, Sidi Bel Abbes, Algeria, Tel. +213556875043; email: nadia_ramdani@ymail.com*
[b]*Hydrology and Materials Laboratory, Faculty of Technology, Djillali Liabes University, Sidi Bel Abbes, Algeria, Tel. +213554576172; email: bounazef@yahoo.com*

Received 14 November 2020; Accepted 7 March 2021

ABSTRACT

The work below is an experimental qualitative study to show the action of a type of natural bentonite, as an adsorbent, on dam water destined for agricultural irrigation and human consumption. The aim is to lower by adsorption 2 parameters, the turbidity to obtain a limpid and clear water, and the nitrates quantity to avoid their transformation into nitrites, which are very toxic to human health and cause damages to the environment. To do this, 3 factors of the adsorbent namely, adsorbent mass, water volume, and adsorption time, on which this water treatment depends, are varied in modelling, in order to observe their action on the obtained results. Then, at the end of the treatment, the reductions of these 2 parameters are formulated by a mathematical formula, describing the turbidity and the nitrates mass in water according to the 3 factors. This permits to note which of the 3 factors is the most preponderant of this treatment, to judge the effectiveness of this method and especially to predict the results concerning the experiments not carried out.

Keywords: Surface water; Groundwater; Adsorption; Turbidity; Nitrate; Experimental design

1. Introduction

The Chorfa dam, located in the Mascara area of the north–west of Algeria, is a collinear water reservoir of medium capacity; it is fed by rainwater to be used for essentially in irrigation of the surrounding fertile lands and human consumption. The stored water, with an average turbidity of approximately 8.9 NTU and an average nitrate content of close to 13 mg/L, does not allow its use directly because rainwater carry alluviums, soil, sand, clay, suspended particles, dissolved organic and inorganic chemical substances. Nitrates are water–soluble and the part not assimilated by plants diffuses and infiltrates into the soil to reach groundwater or surface water. They are easily transformed to nitrites, which are very dangerous to health. It is believed that too high level of nitrates in the aquatic environment induces toxicity on its fauna and flora, modifies the environment (eutrophication) and harms biodiversity. Reducing nitrates, even if it is below the admissible norms (our case), prevents nitrites increase and ameliorates turbidity [1]. It is the nitrates transformation to nitrites can potentially have a negative impact on health. In the blood, the presence of these nitrites causes the formation of "methaemoglobin", a form of

* Corresponding author.

haemoglobin incapable to transport oxygen. On the other hand, the water turbidity of the Chorfa dam is high; this concentration of suspended solids decreases its ecological value [2,3]. For these reasons, filtration and treatment of this water is more than necessary. One carries out a study on the used means to reduce the presence of dissolved nitrates and the turbidity. The treatment is accomplished through adsorption process by bentonite [4,5]; it extracts from the El-Bayadh ore in its natural state without activation or enrichment [6,7]. The descriptive and predictive mathematical modelling is carried out by experimental design; it describes the treatment phenomenon approaching the measured values and at the same time, estimates the results not known experimentally.

2. Study areas and sampling procedures

The sampling of water of Chorfa II dam (Table 1) whose data and characteristics are transmitted to us by Mascara Hydraulics Department. It is located at 65 km north of Mascara city and fed mainly by the Mekerra River, which benefits the dam with a reduced water quantity of 400 mm per year by rainfall.

The necessary sampling measures taken are as follows: (1) Ensure appropriate distance from the rivage. (2) Avoid air bubbles in the bottles. (3) Take samples at a depth of at least 30 cm from the water surface. (4) Collect water with a flow velocity of at least 0.30 m/s. (5) Use opaque vessels. (6) Collect water from three areas at a sufficient distance from each other (Table 2). This is possible using the equipment do available to us by the Mascara Hydraulics Department. This procedure allows the physical method of water filtration by adsorption to be carried out correctly and efficiently by attaching the molecules of the adsorbate to the adsorbent. In contrast to the ultrasonic electrocoagulation method, which enables the element to remove and to separate [8], or the electrochemical method, which removes it by passing an electrical current, similar to electrolysis [9], this method uses another procedure that does not require large means. It is appropriate when the 2 mentioned methods above cannot be applied for technical reasons.

3. Used methods, equipment and apparatuses of analysis and measurements

Turbidity measurements are carried out using a WTW turbid meter. The chosen instrument is a 2100-AN of ISO 7027 standards, which performs measurements by scattering infrared rays at 90°, with a wavelength of λ = 960 ± 30 nm and a nephelometry between 0 and 1,000 NTU. Its scattered light intensity increases each time the concentration of pollutants rises in the water. First, successive reference calibrations are performed with purified water mixed with formazine at different concentrations such as 0.1, 1, 20, 50, 100 NTU. Then, the measurements are done on 3 different samples of samples, taken in the three zones of the Chorfa II dam. The average of the results is 8.83 NTU, that is, more than 5 NTU, which classifies this water, slightly turbid and troubled (Table 2).

The mass of contained nitrates in water is detected with a mass spectrophotometer, type NV 202P. It gives a relatively low value, around 12.83 mg/L. Although the standard of nitrates-NO_3 is 50 mg/L (measured in terms of oxygen and nitrogen), (10 mg/L of nitrates-N, measured in terms of only nitrogen), water is treated to bring it even lower than 12.83 mg/L, because under certain conditions, nitrates are transformed into nitrites, which are salts that are very dangerous to health (for reasons mentioned above). This is added to the already existing nitrites mass, which is 0.176 mg/L, exceeding the norms of 0.1 mg/L.

Table 1
Descriptive table of the dimensions of the Chorfa II dam

Designation	Units	Values
Maximum altitude	m	1,754
Average altitude	m	855
Minimum altitude	m	197.4
Initial capacity without silting	mm^3	83
Reduced capacity after silting	mm^3	70
Average capacity	mm^3	46

Sources: Mascara Hydraulics Department

Table 2
Results of dam water analyses of the 3 sampling zones

Characteristics	Area 1	Area 2	Area 3	Average	Norms
Water *T* (°C)	11.50	10.40	11.5	11.13	25
pH	8.5	8.1	8.25	8.28	9.5 > pH >6.5
Turbidity (NTU)	8.5	8.5	9.5	8.83	5
Nitrates (mg/L)	12.5	12.5	13.5	12.83	50
Nitrites (mg/L)	0.200	0.150	0.180	0.176	0.1
Chlorides (mg/L)	633.5	640.5	650.5	641.5	<500
Sulfates (mg/L)	126.5	125.5	135.5	129.16	500/400
Sodium (mg/L)	219	235	232	228.66	200
Potassium (mg/L)	5	5	6	5.33	12
Calcium (mg/L)	81	79	81	80.33	200
Dissolved oxygen (mg/L)	4.5	4.5	4.7	4.56	5

4. Description and characterization of the natural used bentonite

Natural bentonite with a basic pH of 9.15 is used, of which about 80% of the grains are bigger than 200 μm. The analysis with the copper diffractometer PHILIPS PW1830 (CuK = 1.54060 Å) gives the following spectra in Fig. 1.

The spectrum shows the presence of quartz in the form of SiO_2 at the peak d = 3.35 Å as well as at the secondary reflections (4.29, 2.46, 2.46, 1.81, and 1.54 Å). Calcite is represented by radiations of 3.05, 2.29, 2.09, and 2.9 Å, illite at 10.2 Å, and kaolinite at 4.52 Å. DRX analysis [10,11] shows results that are more refined. The reflection at d = 10 Å (Fig. 2) is due to the no significant illitic phase with other secondary peaks of 5.01 and 3.33 Å. In addition, one observes a ray at 12.36 Å, which is attributed to smectite, and two other rays at 14.16 and 4.74 Å attributed to chlorite.

An infrared spectroscopic analysis [12,13], is done with a Nicolet 410 spectrometer. The obtained spectrum examination [14,15] on the bentonite (Fig. 3) revealed absorption bands, which one presents as follows: (1) Presence of carbonates and other organic impurities (absorption bands located at 1,448 cm^{-1}) characteristic of CO elongations. (2) Presence of quartz (695, 701, and 868 cm^{-1}). (3) The located absorption bands around 3,621; 3,627; 3,743 and 3,749 cm^{-1} represent the presence of illite, while the 1,646 cm^{-1} band characterises the clay (bentonite). The Si–O valence is centred at 1,029 cm^{-1}, while the bands located at 522, 534, and 471 cm^{-1} are attributed to the deformation vibrations of the Si–O–M bonds (M = metal in octahedral position which can be Al, Fe, or Mg).

5. Measurement of turbidity and nitrate quantity after adsorption treatment with bentonite

The study consists in analysing the effect of three factors acting on the two parameters characterising the water quality [16,17], namely, the quantity of adsorbent

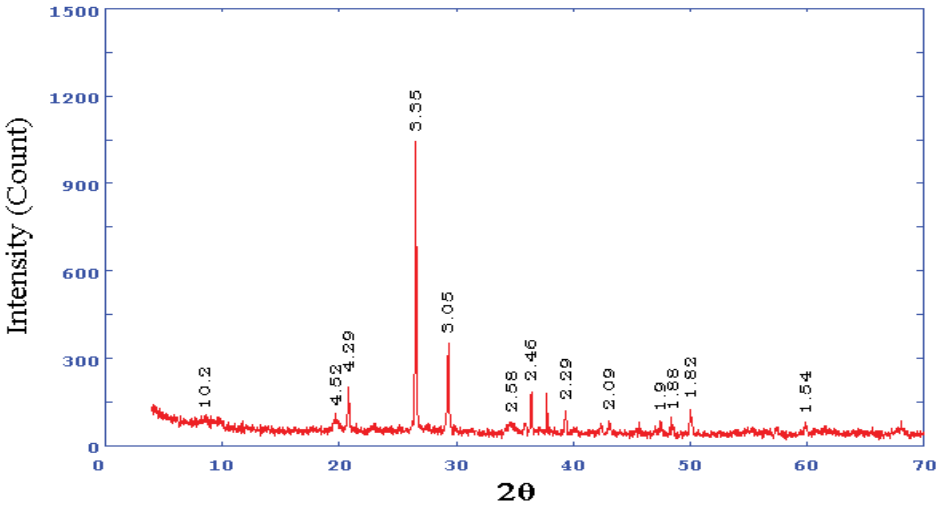

Fig. 1. X-ray diffraction spectrum of used natural bentonite with the inter reticular distances d_{hkl} (Å) (powder diagram).

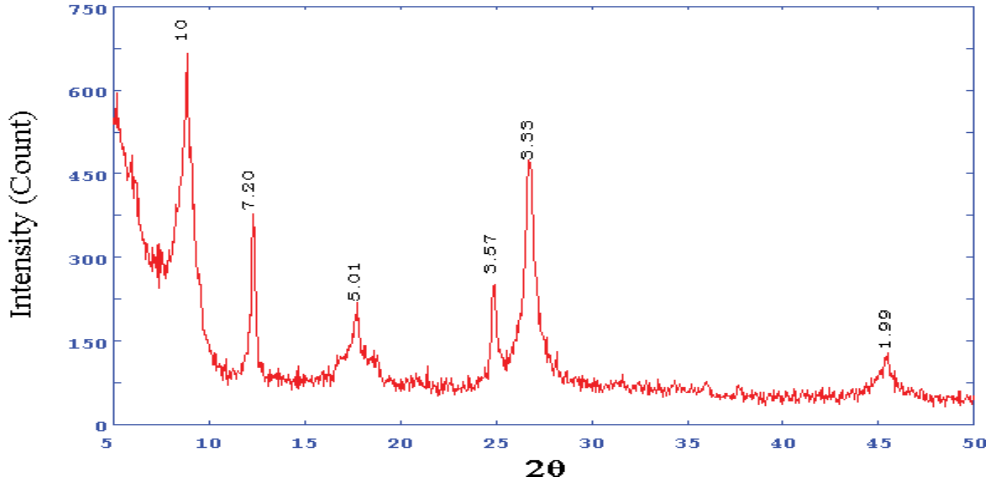

Fig. 2. X-ray diffraction diagram of bentonite clay with distances.

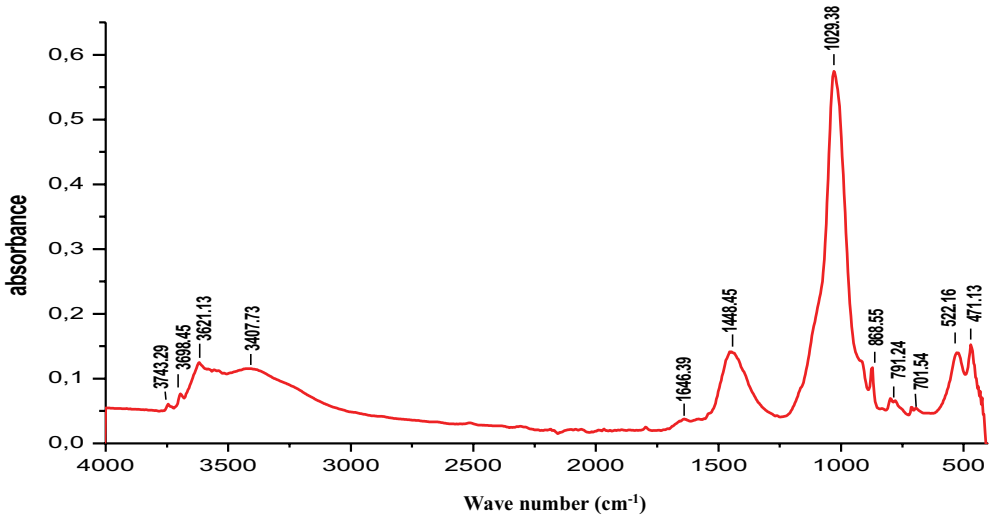

Fig. 3. Infrared spectrum of bentonite.

in g, the used quantity of water for each experiment in mL, and finally the adsorption time in min using non-conventional design of experiments [18,19]. Table 3 shows the results obtained by varying the quantity of bentonite from 2.5 to 10 g, the volume of water from 200 to 500 mL, and the adsorption time with electromagnetic agitation from 15 to 90 min through 9 experiences.

5.1. Measurement and analysis of turbidity results after bentonite treatment

The turbidity (response: y_1) varies according to the combination of the 3 factors x_1, x_2 and x_3, it changes from 0.25 to 0.86 NTU, is therefore significantly lower than the turbidity of the dam water before treatment of 8.83 NTU (Table 2). This behavioural decline is modelled by a mathematical expression chosen in the following linear polynomial form (Eq. (1)) [20]. The following calculation steps are processed using the software "Statistica" and "Modde 6.0" which allow solving a system of 9 equations (form of equation) 1 by matrix calculation. It is obvious that the choice of the 9 experiments is done according to the unconventional design method where the values of the 3 factors are not calculated and predicted in advance, but given by the reality of the fieldwork. In this context, the software identifies and eliminates any aberrant values and reduces the total number of data points at 9 experiments.

$$y_{1_i} = a_0 + a_1x_{1i} + a_2x_{2i} + a_3x_{3i} + a_{12}x_{1i}x_{2i} + a_{13}x_{1i}x_{3i} + a_{23}x_{2i}x_{3i} \quad (1)$$

where x_{ij}: factors in coded form of the three factors acting on turbidity, a_{ij}: coefficients relative to each factor, y_1: response illustrating the true value of turbidity after treatment. The values of x_{ij} must be transformed to coded values without grandeur between –1 and +1 according to Eq. (2) below; x_i is the codded value of the factor, u_{max} is the maximum of the 9 true values, u_{min} is the minimum of the 9 true values, u_i is the true value of the experiment:

$$x_i = \frac{u_i - \left(\frac{u_{max} + u_{min}}{2}\right)}{\left(\frac{u_{max} - u_{min}}{2}\right)} \quad (2)$$

Table 3
Experimental values of parameters after adsorption treatment

Experiment number	Adsorbent mass (g) (x_1)	Water volume (mL) (x_2)	Adsorption time (min) (x_3)	Turbidity NTU (y_1)	Nitrates quantity mg/L (y_2)
1	2.5	300	30	0.86	9.57
2	5	300	30	0.75	6.58
3	10	300	30	0.50	4.6
4	2.5	200	30	0.25	2.98
5	2.5	200	60	0.25	1.09
6	2.5	200	90	0.30	1.08
7	5	250	15	0.39	10.1
8	5	400	15	0.40	22.3
9	5	500	15	0.38	27.47

These coded values (x_i), without units, are used in Eq. (1) and combined with the true turbidity values to form a system of 9 equations (Table 4) [21].

The matrix calculation of the coefficients a_{ij}, from the 9 equations, does by the following well-known expression [22].

$$a_i = \left(X^t X\right)^{-1}\left(X^t\right)\left(Y\right) \tag{3}$$

where X is model Matrix. X^t is the transpose matrix. $(X^tX)^{-1}$ is information matrix. The coefficients of the model are show in Table 5.

This is what allows us to write the final form of the model showing the descriptive and predictive turbidity variation as a function of 3 factors; it shows by Eq. (4):

$$y = 0.855094 + 0.015795x_1 + 0.168515x_2 + 0.46479x_3 - 0.589651x_1x_2 + 0.501452x_1x_3 + 0.0458737x_2x_3 \tag{4}$$

This mathematical model has several advantages since it has a simple form with no difficult functions, it is both descriptive and predictive, and interacts between the 3 factors. At first view, one observes that the most preponderant coefficient is a_{12}; it acts proportionally on the coded values of the mass of the adsorbent (M_{ads}) and on the volume of water (V_{wat}). However, it is necessary to associate these coefficients a_{ij} with the coded values of the factors x_{jj} in order to know the effect of each term of the model for each experiment on the turbidity. It is illustrated by two quality indicators, the first is descriptive coefficient ($R^2 = 0.998$); it belongs to the interval $0 < R^2 \leq +1$, and it is very close to +1, this coefficient is largely satisfying. The other one, ($Q^2 = 0.982$) is predictive indicator, it belongs to the interval $-\infty \leq Q^2 \leq +1$, which shows that the turbidity previsions are close to reality. Table 6 and Fig. 4 show precisely the differences between the measured values and the predicted values. These differences vary between 0.42% for the third measurement and 3.33% for the fourth measurement. Only the fifth measurement diverges from the admissible deviation. Below (Fig. 5), they are response surfaces and contours of the predictive values. They show how the water turbidity after treatment with bentonite by adsorption varies as a function of the three factors x_{jj} and their interactions. The used software gives us from the figures all predicted turbidity values witch are within the experimental work domain for 3 values of adsorption time, which are 15, 52.5 and 90 min.

Table 7 shows 15 values predicted by the model, in which the smallest theoretical value of ≈0 NTU is obtained by combining 6.15 g of adsorbent, 350 mL of dam water, and 15 min of adsorption time. On the other hand, the maximum value of 5.11 NTU is obtained by accommodating the values of 10 g of bentonite, 250 mL of treated water, and 90 min of adsorption time. By analysing the contours, one sees that for an adsorption time of 15 min, the contours

Table 4
Coded values of the 3 factors x_i acting on the response y

Experiment number	Coded adsorbent mass	Coded water volume	Coded adsorption time
1	–1	–0.333	–0.6
2	–0.333	–0.333	–0.6
3	1	–0.333	–0.6
4	–1	–1	–0.6
5	–1	–1	0.2
6	–1	–1	1
7	–0.333	–0.667	–1
8	–0.333	0.333	–1
9	–0.333	1	–1

Table 5
Coefficients values of polynomial model

Factors	Monomials coefficients	Coefficients values of polynomial
Constant	a_0	0.855094
M_{ads} (x_1)	a_1	0.015795
V_{wat} (x_2)	a_2	0.168515
T_{ads} (x_3)	a_3	0.46479
$M_{ads} \times V_{wat}$ (x_1x_2)	a_{12}	–0.589651
$M_{ads} \times T_{ads}$ (x_1x_3)	a_{13}	0.501452
$V_{wat} \times T_{ads}$ (x_2x_3)	a_{23}	0.0458737

Table 6
Deviation values between observed and predicted values

Experiment number	Measured values	Predicted values	Deviations $V_{obs} - V_{pred}$
1	0.86	0.864286	–0.00428569
2	0.75	0.743572	0.00642848
3	0.5	0.502143	–0.00214291
4	0.25	0.241667	0.00833338
5	0.25	0.266667	–0.0166667
6	0.3	0.291667	0.00833341
7	0.39	0.394211	–0.00421059
8	0.4	0.389474	0.0105263
9	0.38	0.386316	–0.00631589

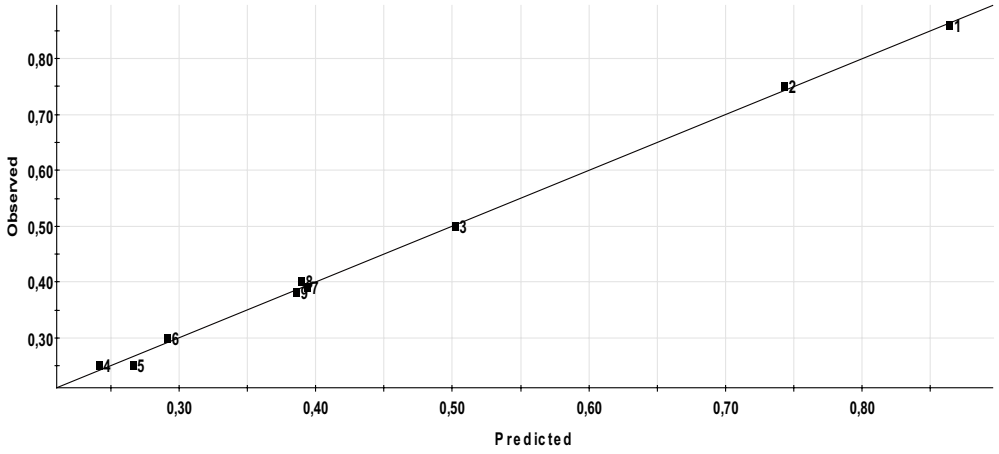

Fig. 4. Deviations of experiment points at the regression line.

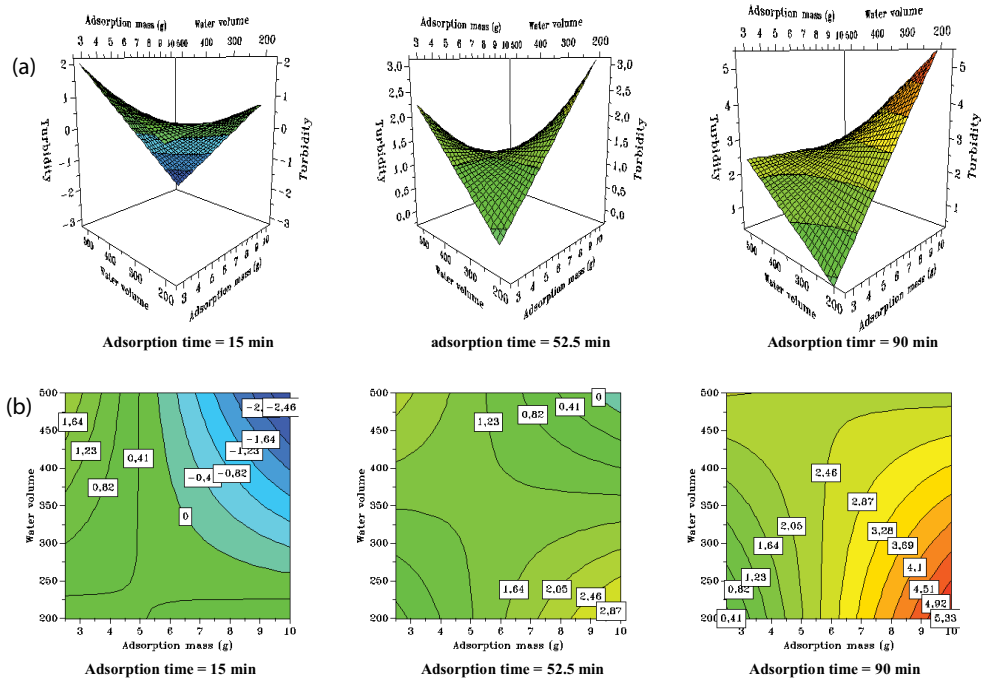

Fig. 5. (a) Predictive and illustrative response surfaces of the model and (b) illustrative and predictive contours of the model.

Table 7
Examples of turbidity predictions from the model (contours and surfaces) according to the 3 factors

No.	Adsorbent mass (g)	Water volume (mL)	Adsorption time (min)	Turbidity (NTU)
1	3	250	15	0.500
2	2.5	200	15	0.234
3	3	250	90	0.935
4	4	300	15	0.566
5	2.5	200	52.5	0.266
6	4	300	90	1.690
7	5	350	15	0.393
8	2.5	200	90	0.298
9	5	350	90	2.210
10	6	400	52.5	1.240
11	6	400	90	2.490
12	7	450	52.5	0.930
13	7	450	90	2.530
14	9	500	52.5	0.0391
15	9	500	52.5	2.230

are practically vertical, oriented to the top, which shows that for a given adsorbent mass, the treated water volume increase has very few effect, and the turbidity remains constant.

The same is true for the 90 min adsorption process, in which the curves are directed downwards, this indicate that for a given adsorbent mass, the water volume decrease causes an insignificant change in turbidity, meanwhile it remains almost constant.

On the opposite, for the case of the adsorption time of 52.5 min, the contours give a star form, sometimes it is the adsorbent mass that remains few active (part of the horizontal contours), sometimes, it is the treated water volume that remains few laborious (part of the vertical contours).

One also notes from the Table 7 and Fig. 5 that for the same adsorbent mass and the same water quantity, the turbidity decreases with the reduction of the adsorption time. It also decreases if the adsorption mass is reduced while keeping the same adsorption time and the same volume. This is not valid for the volume of 500 mL, where the opposite occurs; it probably explains by the increase in volume and time simultaneously.

Negative values of turbidity remain only theoretical approximations by extension, calculated by the model; they have no correct physical significance. Another type of analysis is done; it gives the possibility to see how it changes according to only factor while keeping two others invariable. Our choice is based on three distinct factor values, the minimum, the mean and the maximum values.

5.1.1. First case, minimum values: absorbent mass = 2.5 g – water volume = 200 mL – adsorption time = 15 min

Inversely, to the action of the cases of the interactions between factors x_{ij} (Fig. 6), one notes that taken separately, at their minimum value, all three, increase turbidity but in different manners.

It is the increase in the water volume, which has a significant tendency in the first figure (Fig. 6b), when the 2 others take their minimum value, whereas the adsorption time has very little effect on turbidity under the same conditions mentioned above (Fig. 6c).

5.1.2. Second case, median values: absorbent mass = 6.250 g – water volume = 350 mL – adsorption time = 52.5 min

In Fig. 7, only the water volume curve reverses from Fig. 6, as the increase in this factor reduces turbidity when the 2 other have their mean value. The other 2 curves give the same effect as the first case with a different tendency, slower for Fig. 7a, and quicker for Fig. 7c. Therefore, an average water volume of 350 mL reverses the tendency; it reduces the turbidity.

5.1.3. Third case, maximum values: absorbent mass = 10 g – water volume = 500 mL – adsorption time = 90 min.

At the maximum of the 3 factors values (Fig. 8), only the adsorption time (Fig. 8c) retains its action on turbidity increasing, the first 2 factors (Figs. 8a and b) reverse it and lower it in comparison with the first case. Whatever its value, the adsorption time increases always turbidity (Figs 6, 7 and 8c). Below, one presents in Table 8, some predicted values that give (by the model) a turbidity that tends theoretically towards zero and show that the water is clear and limpid after treatment with bentonite (5 NTU ≥ turbidity).

Student test shows that 6 of the 7 coefficients a_{ij} are significant in the polynomial. Only a_1 remains below t_{crit} × Si = 0.025845414, which means that it does not

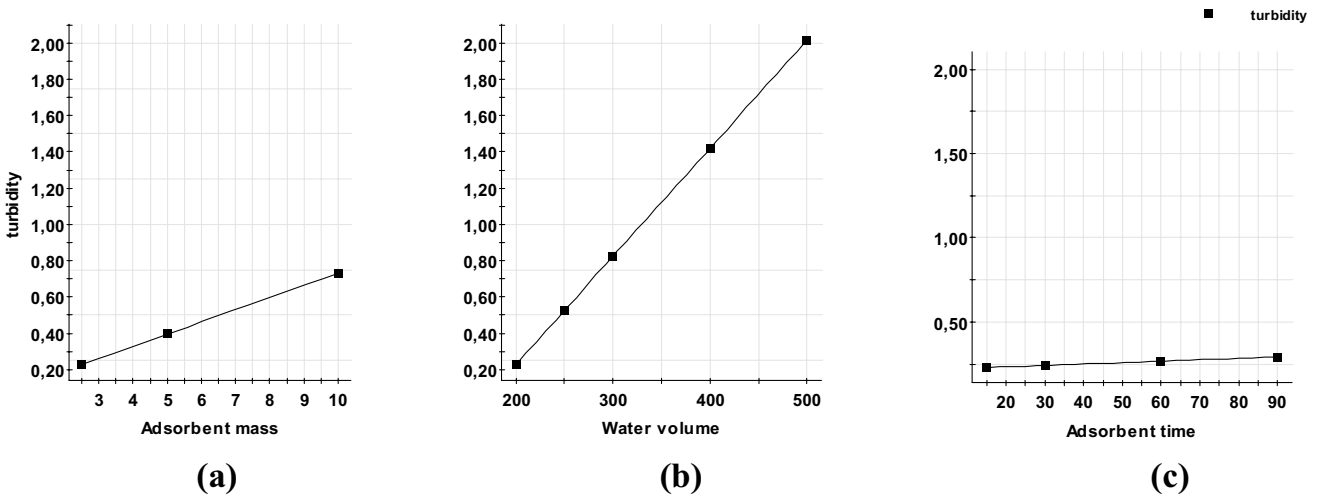

Fig. 6. Turbidity variation for minimum factor values.

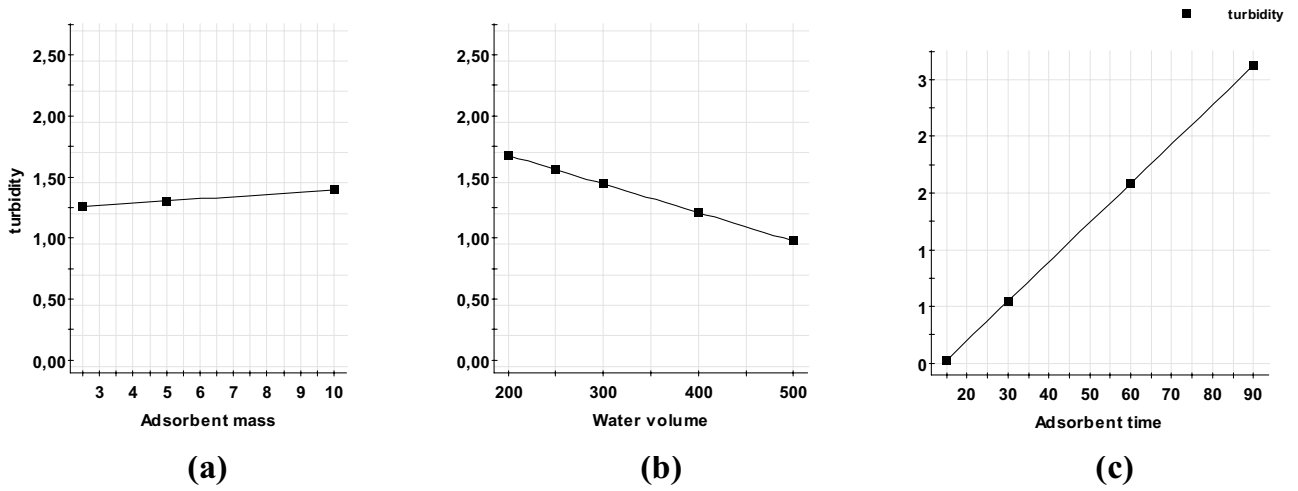

Fig. 7. Turbidity variation for median factors values.

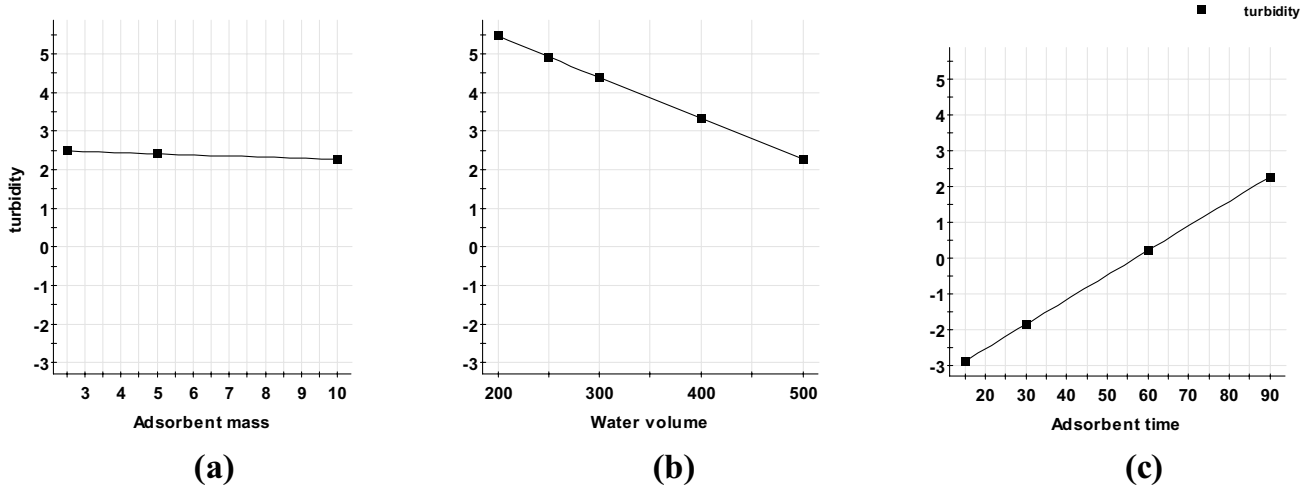

Fig. 8. Turbidity variation for maximum factor values.

Table 8
Predicted values predicted by the model of the 3 parameters allowing to approach zero NTU of turbidity

No.	Adsorption time (min)	Adsorbent mass (g)	Water volume (mL)	Turbidity (NTU)
1	15	6.55	330	0.000259
2	52.5	9.45	480	0.000161
3	15	9.20	268	0.00124
4	30	6.58	495	0.00623
5	15	5.55	495	–0.00973

act in a preponderant manner compared to the others. The action of the 6 other coefficients is more dominant on the turbidity, which demonstrates once again that the model is significant.

The Fisher–Snedecor test shows that the critical Fisher number F_{crit} = 19.330, which describes the interactions of the factors is lower than the observed number F_{obs} = 191.645, the model is acceptable with 5% of risk, that this will not happen. The statistical study of water turbidity by the design of experiments method is fully completed.

The model describing this parameter under the influence of the 3 factors is therefore acceptable as showed by the 2 tests. In summary, (a) for a minimum adsorption time of 15 min, below V_{wat} ≈ 230 mL, the increase of the adsorption mass increases the turbidity, beyond that, it decreases it. Below the bentonite mass, M_{ads} ≈ 5 g, the water volume increase raises the turbidity, while above it decreases it. (b) For a median adsorption time of 52.5 min, below V_{wat} ≈ 365 mL, the increase in the adsorbent mass deteriorates the turbidity, above, it progresses it. Below the mass of bentonite M_{ads} ≈ 5.4 g, the water volume increase degrades the turbidity, whereas above, it improves it. (c) For a maximum adsorption time of 90 min, below V_{wat} ≈ 487 mL, the augmentation in the adsorption mass clarifies the water, and vice-versa. Below M_{ads} ≈ 2.6 g of bentonite, the increase in water volume improves the turbidity while above, it aggravates it.

5.2. Measurement and analysis of nitrates quantity results after bentonite treatment

Based on Table 3, the modelling of the quantity of dissolved nitrates in water is done following the same steps as for turbidity. The coded values, deduced by formula 2, acting on the response y (quantity of nitrates), and ranging from –1 to +1, are given in Table 9.

Matrix calculation gives the coefficients a_{ij} shown in Table 10; the mathematical model therefore takes the form of Eq. (5).

$$y = 5.60818 - 2.52048x_1 + 3.89066x_2 - 9.51192x_3 - 2.00185x_1x_2 - 5.53582x_1x_3 - 4.60904x_2x_3 \quad (5)$$

This polynomial (5) represents the mathematical model of the nitrates presence in the water after treatment under the influence of 3 factors x_i and their interactions x_ix_j. This form gives very realistic estimated quality indicators, as close to +1, one descriptive R^2 = 0.995 and other predictive Q^2 = 0.964 and gives illustrated deviations in Fig. 9. The response surfaces (Fig. 10a) and contours

Table 10
Values of the coefficients of the polynomial model

Factors	Coefficients	Coefficients values
Constant	a_0	5.60818
M_{ads} (x_1)	a_1	–2.52048
V_{wat} (x_2)	a_2	3.89066
T_{ads} (x_3)	a_3	–9.51192
$M_{ads} \times V_{wat}$ (x_1x_2)	a_{12}	–2.00185
$M_{ads} \times T_{ads}$ (x_1x_3)	a_{13}	–5.53582
$V_{wat} \times T_{ads}$ (x_2x_3)	a_{23}	–4.60904

Table 9
Coded values of the 3 factors x_i acting on the response y

Number	Adsorbent mass	Water volume	Adsorption time
1	–1	–0.333	–0.6
2	–0.333	–0.333	–0.6
3	1	–0.333	–0.6
4	–1	–1	–0.6
5	–1	–1	0.2
6	–1	–1	1
7	–0.333	–0.667	–1
8	–0.333	0.333	–1
9	–0.333	1	–1

(Fig. 10b) show how the nitrates quantity in the water after bentonite treatment varies according to the 3 factors x_i and their interactions $x_i x_j$. The given values of the times above 52.5 min of dissolved nitrates are negative and purely theoretical; they do not represent true cases. The contours in Fig. 10 are of distinct types, almost horizontal for the adsorption time of 15 min, and almost vertical for the time of 52.5 min.

In the first case (Fig. 10b, T_{ads} = 15 min), this indicates that the increase in adsorbent mass has very little influence on the presence of nitrates (approximately horizontal contours), whereas in the second (Fig. 10b, T_{ads} = 52.5 min) it is the increase in water volume, which remains without any noticeable influence (approximately vertical contours).

From this, one notes some predicted values by the model, which shows us that it is the increase in adsorption time combined with the decrease in water volume or the increase in adsorbent mass that causes the nitrates fall in water (Table 11).

However, the influence of the factors taken in isolation on the presence of nitrates acts differently than when there is an interaction between them; the graphs below show this:

5.2.1. First case, minimum values: absorbent mass = 2.5 g – water volume = 200 mL – adsorption time = 15 min

The first graph in Fig. 11a shows that for a minimum water volume of 200 mL and a minimum adsorption time

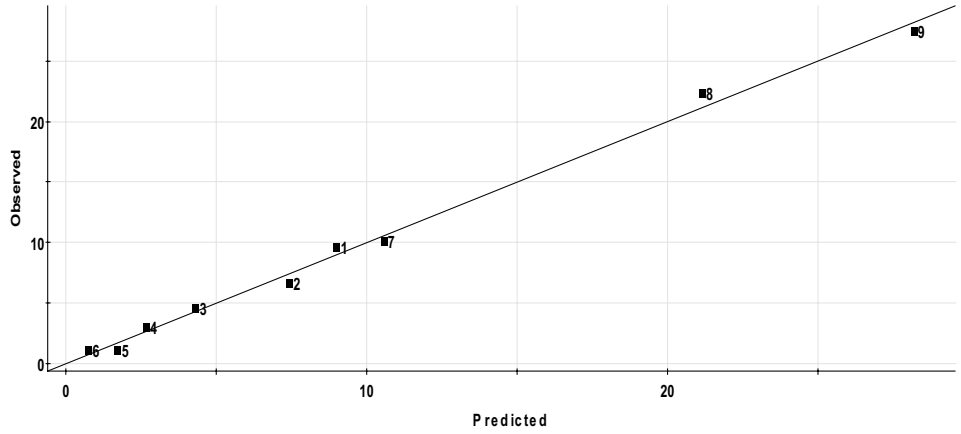

Fig. 9. Illustration of the deviations from the regression line.

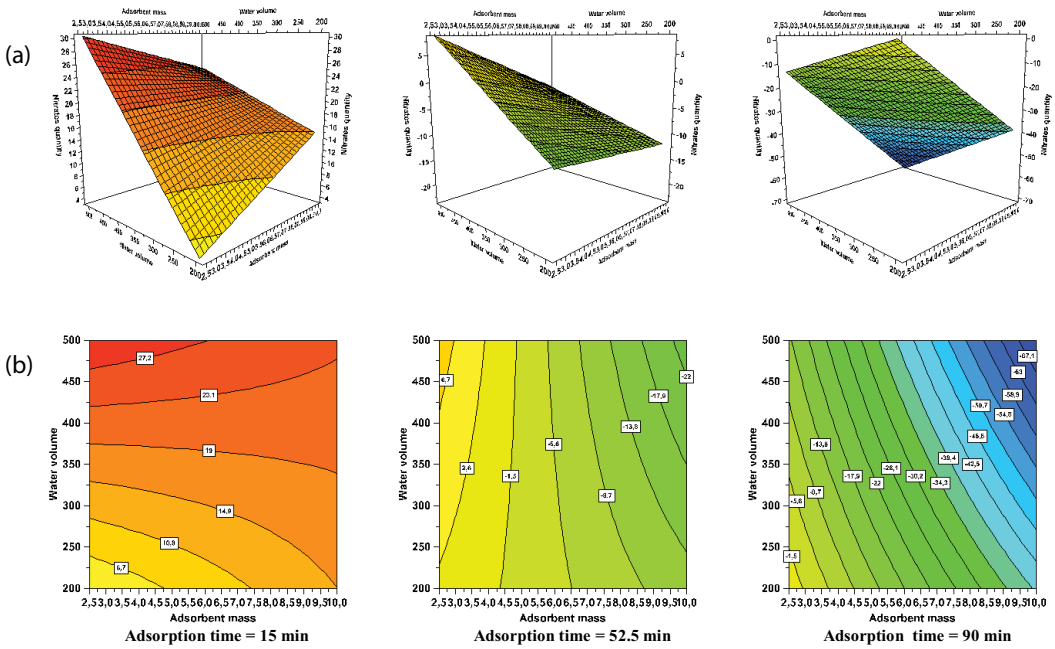

Fig. 10. (a) Illustrative and predictive response surfaces of the presence of nitrates and (b) illustrative and predictive contours of the nitrates presence.

of 15 min (constant), the nitrates quantity increases linearly with the increase in mass of the absorbent. On the second graph (Fig. 11b), the mass of the absorbent kept at 2.5 g and the adsorption time at 15 min, here too, the increase in the volume of treated water increases the quantity of nitrates, but with a pronounced increasing tendency. On the other hand, on the third graph (c), while keeping the mass of the adsorbent at 2.5 g and the volume of water at 200 mL (invariable), the presence of nitrates falls, the mathematical tendency curve is the weakest of the 3 graphs.

5.2.2. Second case, average values: absorbent mass = 6.250 g – water volume = 350 mL – adsorption time = 52.5 min

In this second case (Fig. 12), where the 2 mentioned average values of each factor are kept to vary the 3rd, one sees the inverse effect of the 2 first curves in Figs. 11a and b, since they are decreasing, while the decreasing tendency of the third curve becomes more increased. For their average values, the increase of all factors decreases the nitrates quantity dissolved in the treated dam water.

5.2.3. Third case, maximum values: absorbent mass = 10 g – volume of water = 500 mL – adsorption time = 90 min

Keeping the factors in their maximum values (Fig. 13), the behaviour remains the same as in the 2nd case, with the difference that the linear decrease in the presence of nitrates in the treated water is faster than before. In the end, the nitrates quantity in the water varies according to the three factors. (a) For an adsorption time of 15 min, if the volume of water is less than 394 mL, the quantity of dissolved nitrates increases with the increase of the adsorbent mass. On the other hand, if V_{wat} > 394 mL, it is the opposite which occurs. (b) For an adsorption time of 52.5 min, the increase

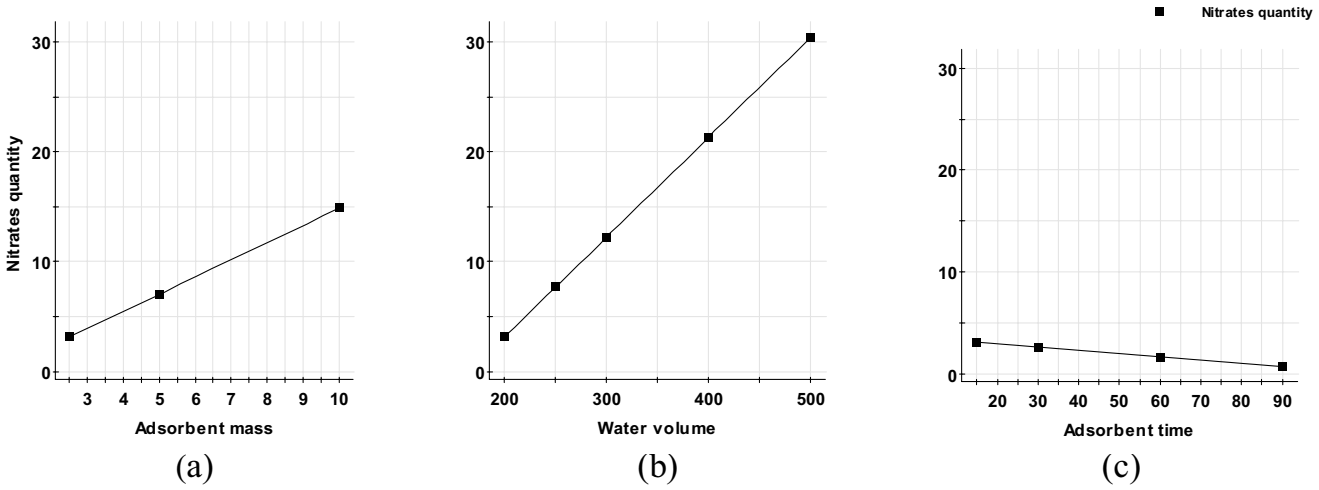

Fig. 11. Variation in the quantity of nitrate for minimum factors values.

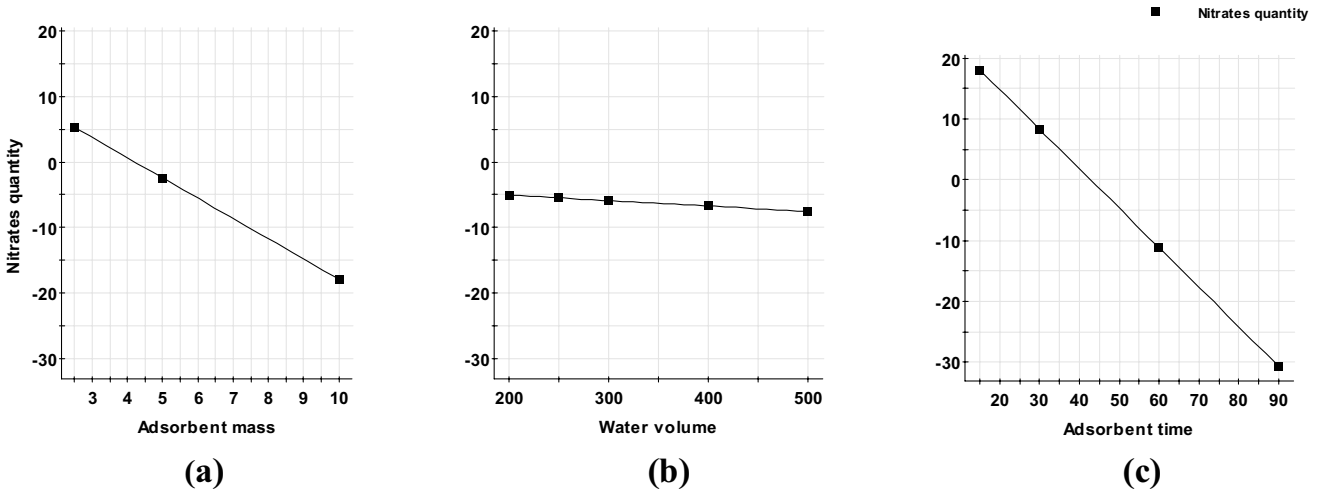

Fig. 12. Variation in the quantity of nitrates for the average values of the 3 factors.

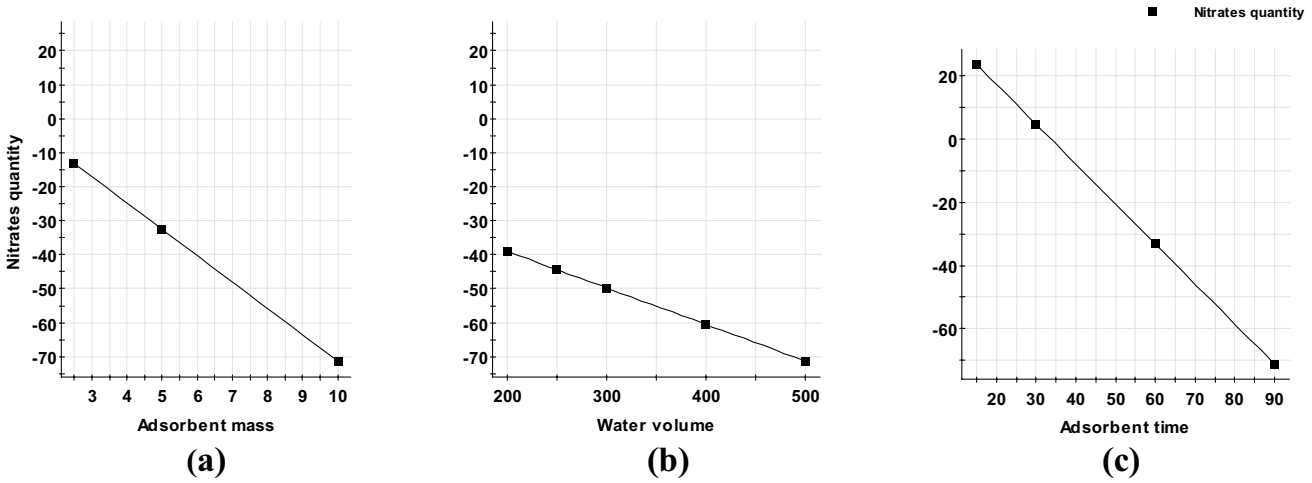

Fig. 13. Variation in nitrates quantity for the maximum values of the 3 factors.

Table 11
Predictive values from the model as a function of the 3 factors

No.	Absorbent mass (g)	Water volume (mL)	Adsorption time (min)	Nitrates quantity (mg/L)
1	3	200	15	4.15
2	3	500	15	29.9
3	6.5	200	15	12.3
4	6.5	500	15	26.9
5	10	200	15	14.8
6	10	500	15	23.8
7	3	200	52.5	1.01
8	3	500	52.5	6.49
9	6.5	200	52.5	–5.52

in the mass of adsorbent reduces the nitrates quantity inside the treated water over the completely measuring domain. It is at the border of the mass of 5.5 g of bentonite that a change of behaviour is observed. If it is lower, the quantity of nitrates increases with the increase of the used water volume and vice versa if it is higher. (c) The adsorption time of 90 min does not reflect the true cases, it gives purely theoretical negative values of nitrates presence, it is therefore not considered.

6. Conclusion

Variations of turbidity and the dissolved mass of nitrates are function of three mentioned different factors in the study, But they become complex with their interactions. The two models found, the contours and the response surfaces illustrate this. Turbidity and nitrate mass are independent of each other. It is not the choice of three factors that decrease turbidity witch gives automatically the ideal decrease of water nitrates. Therefore, the choice do for each adsorption treatment separately using one of the proposed solutions of the mathematical models. This method remains good and gives satisfactory results in laboratories; it can be applied without difficulties in the industrial domain.

Acknowledgments

Our thanks go to the 2 research laboratories, as well as to Mascara's Hydraulics Department, which helped us with some data and information.

References

[1] H. Gökçekuş, Special issue on the 2nd International Conference on Water Problems in the Mediterranean Countries (WPMC) 6–10 May 2019, Lefkosa, Turkish Republic of Northern Cyprus, 2020, pp. 236–236.
[2] M. Triwiswara, C.-G. Lee, J.-K. Moon, S.-J. Park, Adsorption of triclosan from aqueous solution onto char derived from palm kernel shell, Desal. Water Treat., 177 (2020) 71–79.
[3] H. Hashtroudi, Treatment of lead contaminated water using lupin straw: adsorption mechanism, isotherms and kinetics studies, Desal. Water Treat., 182 (2020) 155–167.
[4] B. Ghiasi, M.H. Niksokhan, A.M. Mazdeh, Co-transport of chromium(VI) and bentonite colloidal particles in water-saturated porous media: effect of colloid concentration, sand gradation, and flow velocity, J. Contam. Hydrol., 234 (2020) 103682, doi: 10.1016/j.jconhyd.2020.103682.
[5] B. Liao, Y.Y. Li, Y. Guan, Y.H. Liu, Q.Q. Huang, C.W. Ye, G. Liu, F. Xu, Insight into barrier mechanism of fly ash-bentonite blocking wall for lead pollution in groundwater, J. Hydrol., 590 (2020) 125444, doi: 10.1016/j.jhydrol.2020.125444.

[6] L. Peng, B. Chen, Y.X. Zhao, Quantitative characterization and comparsion of bentonite microstructure by small angle X-ray scattering and nitrogen adsorption, Constr. Build. Mater., 262 (2020) 120863, doi: 10.1016/j.conbuildmat.2020.120863.
[7] R.F. Resende, P.V. Brandão Leal, D.H. Pereira, Z.M. Magriotis, Removal of fatty acid by natural and modified bentonites: elucidation of adsorption mechanism, Colloids Surf., A, 605 (2020) 125340, doi: 10.1016/j.colsurfa.2020.125340.
[8] S. Al-Marri, S.S. AlQuzweeni, K.S. Hashim, R. Al Khaddar, P. Kot, R.S. Al Kizwini, S.L. Zubaidi, Z.S. Al-Khafaji, Ultrasonic-electrocoagulation method for nitrate removal from water, Mater. Sci. Eng., 888 (2020) 012073.
[9] M. AL-Housni, A.H. Hussein, D. Yeboah, R. Al Khaddar, B. Abdulhadi, A.A. Shubbar, K.S. Hashim, Electrochemical removal of nitrate from wastewater, Mater. Sci. Eng., 888 (2020) 012037.
[10] B.M. Butler, J. Palarea-Albaladejo, K.D. Shepherd, S. Hillier, Mineral–nutrient relationships in African soils assessed using cluster analysis of X-ray powder diffraction patterns and compositional methods, Geodermal, 375 (2020) 114474, doi: 10.1016/j.geoderma.2020.114474.
[11] X.M. Ke, Z.F. Wu, J.Z. Lin, D.K. Zhang, A rapid analytical method for the specific surface area of amorphous SiO_2 based on X-ray diffraction, J. Non-Cryst. Solids, 531 (2020) 119841, doi: 10.1016/j.jnoncrysol.2019.119841.
[12] O. Sivrikaya, B. Uzal, Y.E. Ozturk, Practical charts to identify the predominant clay mineral based on oxide composition of clayey soils, Appl. Clay Sci., 135 (2017) 532–537.
[13] X. Zhou, D. Liu, H.L. Bu, L.L. Deng, H.M. Liu, P. Yuan, P.X. Du, H.Z. Song, XRD-based quantitative analysis of clay minerals using reference intensity ratios, mineral intensity factors, Rietveld, and full pattern summation methods: a critical review, Solid Earth Sci., 3 (2018) 16–29.
[14] J. Środoń, Chapter 12.2 – Identification and Quantitative Analysis of Clay Minerals, in: Developments in Clay Science, Elsevier, Amsterdam, 2006, pp. 765–787.
[15] H.B. Deng, Y. Wu, I. Shahzadi, R. Liu, Y. Yi, D. Li, S.Y. Cao, C. Wang, J. Huang, H.Y. Su, Chapter 8 – Nanomaterials From Mixed-Layer Clay Minerals: Structure, Properties, and Functional Applications, A.Q. Wang, W.B. Wang, Eds., Nanomaterials from Clay Minerals: A New Approach to Green Functional Materials Micro and Nano Technologies, 2019, pp. 365–413.
[16] H.Q. Wang, J.T. Hu, W. Wan, H.Q. Gui, F.H. Qin, F.J. Yu, J.G. Liu, L. Lü, A wide dynamic range and high resolution all-fiber-optic turbidity measurement system based on single photon detection technique, Measurement, 134 (2019) 820–824.
[17] J.W. Li, Y.F. Tong, L. Guan, S.F. Wu, D.B. Li, A turbidity compensation method for COD measurements by UV–vis spectroscopy, Optik, 186 (2019) 129–136.
[18] A. Rymszewicz, J.J. O'Sullivan, M. Bruen, J.N. Turner, D.M. Lawler, E. Conroy, M. Kelly-Quinn, Measurement differences between turbidity instruments, and their implications for suspended sediment concentration and load calculations: a sensor inter-comparison study, J. Environ. Manage., 199 (2017) 99–108.
[19] L. Yang, J. Wang, S.S. Wang, Y.P. Liao, Y. Li, A new method to improve the sensitivity of nitrate concentration measurement in seawater based on dispersion turning point, Optik, 205 (2020) 164202, doi: 10.1016/j.ijleo.2020.164202.
[20] J. Goupy, Methods for Experimental Design: Principles and Applications for Physicists and Chemists, Elsevier, Amsterdam, 1993, p. 449.
[21] J. Goupy, Introduction at the Design of Experiments, with Applications, 5th ed., Dunod Edition, Paris, 2005
[22] A. Djeffal, S.E. Bendaoudi, M. Bounazef, E.A.A. Bedia, Behavioural modelling of lips seal made with polytetrafluoroethylene enriched by glass fibers, Modell. Numer. Simul. Mater. Sci., 3 (2013) 170–174.